

# Aminoalkylbis(phosphonates): Their Complexation Properties in Solution and in the Solid State

Vojtěch Kubiček,<sup>\*,[a]</sup> Jan Kotek,<sup>[a]</sup> Petr Hermann,<sup>[a]</sup> and Ivan Lukeš<sup>[a]</sup>

**Keywords:** Phosphonates / Complexation / Stability constants / Potentiometry

Five geminal bis(phosphonates) containing an amino group in the  $\alpha$ ,  $\gamma$  or  $\delta$  position of the carbon chain have been synthesised and their acid–base and complexation properties with  $\text{Cu}^{2+}$ ,  $\text{Zn}^{2+}$ ,  $\text{Ca}^{2+}$ ,  $\text{Mg}^{2+}$  and  $\text{Na}^+$  ions studied by potentiometry. Determination of the stability constants of the complexes with divalent metal ions is complicated by the formation of precipitates. The results of these studies show a negligible effect of the hydroxo group in the  $\alpha$  position on the acid–base and complexation properties of the ligands. The presence of an amino group in the  $\alpha$  position, however, decreases the basicity, which results in a lower complexation ability of the

bis(phosphonates). The crystal structures of the three ligands with different degrees of protonation have also been determined. The structure of the triammonium salt of aminomethylbis(phosphonic acid) shows that the proton is bound to the nitrogen atom in monoprotonated species. The structure of the  $\text{Cu}^{2+}$  complex of pamidronate  $[\{\text{Cu}_2(\text{H}_2\text{pam})_2\} \cdot \text{H}_2\text{O}]_n$  shows the presence of dimeric units with a relatively short distance (2.99 Å) between the metal centres. These units form a coordination polymeric chain.

(© Wiley-VCH Verlag GmbH & Co. KGaA, 69451 Weinheim, Germany, 2007)

## Introduction

Pyrophosphate is an important regulator of calcium metabolism in living organisms. Replacement of the bridging oxygen atom of pyrophosphate with methylene or a substituted methylene group results in the formation of geminal bis(phosphonic acids), hereafter referred to simply as bis(phosphonates). This group of compounds has been intensively studied over the last fifty years. As the central carbon atom can be substituted with many different organic groups, a huge number of bis(phosphonates) have been synthesised. Their low toxicity, high biological stability (they are not metabolized) and high affinity for calcium and calcified tissues have made them suitable for many biomedical applications.<sup>[1]</sup> After adsorption on the bone surface, bis(phosphonates) can affect the functioning of bone cells such as osteoclasts and osteocysts, which are responsible for bone formation and desorption. Because of this, bis(phosphonates) can be used in the treatment of osteoporosis, Paget disease and other diseases of calcified tissues. The large variability of bis(phosphonates) provides a wide scope of therapeutic effects, and some of the bis(phosphonates) used therapeutically nowadays are shown in Table 1. Bis(phosphonates) form complexes with divalent and trivalent transition metal ions, and these complexes have been applied in bone radiotherapy and for palliation of pain associated with metastatic bone cancer.<sup>[1]</sup>

Recently, attention has been paid to tissue-specific imaging and therapy. Attachment of a biologically active molecule to a molecule of contrast agent results in the binding of such species to specific tissue and increases their local concentration. This provides a better contrast and leads to the use of lower doses of the contrast agents and therapeutic agents. In these applications, bis(phosphonates) can play the role of a targeting group as their conjugate with the medically active molecule can be swiftly and strongly adsorbed on the surface of bones and other calcified tissues.<sup>[2,3]</sup> Recently, we have contributed to this field by studying the bis(phosphonate)-modified macrocyclic ligand  $\text{H}_4\text{dota}$  (1,4,7,10-tetraazacyclododecane-1,4,7,10-tetraacetic acid), which is useful for targeted visualisation of calcified tissues by magnetic resonance imaging (MRI) or other radiodiagnostic/therapeutic treatment.<sup>[4]</sup>

Most of the clinically used bis(phosphonates) contain an amino group in the carbon chain. These aminoalkylbis(phosphonates) strongly complex transition metal ions. Despite this fact, only a few studies have concentrated on their acid–base and complexation properties,<sup>[5–13]</sup> and generally only protonation constants have been determined. In the case of some ligands, their complexing behaviour with  $\text{Cu}^{2+}$  ions has also been studied.<sup>[5,6,11,13]</sup> Unfortunately, the reported results are not always consistent. Some of the dissociation/protonation constants are beyond the lower or higher limits of the applied methods and, therefore, they were not determined. Furthermore, most of the studies were performed in presence of  $\text{Na}^+/\text{K}^+$  ions.<sup>[5,6,9–13]</sup> As these ions are complexed by the bis(phosphonates),<sup>[14,15]</sup> all reported values of dissociation/protonation and complex stability

[a] Department of Inorganic Chemistry, Charles University, Hlavova 8, 12840 Prague 2, The Czech Republic  
E-mail: vvvojta@volny.cz

Supporting information for this article is available on the WWW under <http://www.eurjic.org> or from the author.

Table 1. Bis(phosphonates)  $[R^1R^2C(PO_3H_2)_2]$  used in medical practice.

Commercial name	$-R^1$	$-R^2$	Commercial name	$-R^1$	$-R^2$
Aledronate	$-\text{OH}$	$-(\text{CH}_2)_3-\text{NH}_2$	Pamidronate	$-\text{OH}$	$-(\text{CH}_2)_2-\text{NH}_2$
Clodronate	$-\text{Cl}$	$-\text{Cl}$	Risedronate	$-\text{OH}$	$-\text{CH}_2-\text{C}_6\text{H}_4-\text{N}$
Etidronate	$-\text{OH}$	$-\text{CH}_3$	Tiludronate	$-\text{H}$	$-\text{S}-\text{C}_6\text{H}_4-\text{Cl}$
Ibandronate	$-\text{OH}$	$-(\text{CH}_2)_2-\text{N}(\text{CH}_3)(\text{CH}_2)_4-\text{CH}_3$	Zoledronate	$-\text{OH}$	$-\text{CH}_2-\text{N}(\text{CH}_3)-\text{C}_6\text{H}_4-\text{N}$

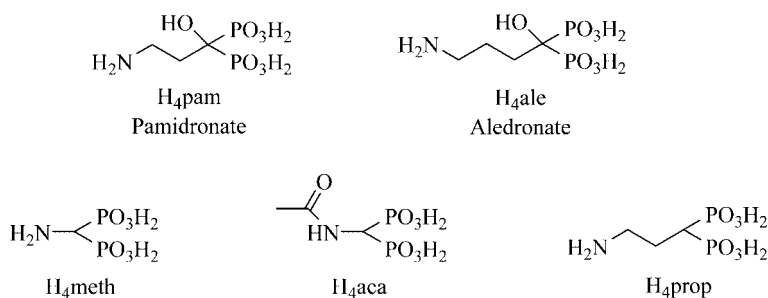


Figure 1. Structures of the ligands discussed.

constants are disturbed by the formation of such complexes.

In light of this we decided to use the non-complexing tetramethylammonium cation in the supporting electrolyte to avoid alkali metal complex formation. In this work, we report on the results of a solution study of four bis(phosphonates) containing an amino group in the side chain. Furthermore, as the bis(phosphonate) moiety is often connected by a peptidic bond in the bifunctional ligands, we chose a new amide derivative **H<sub>4</sub>aca** as a model compound for comparison (Figure 1). The protonation constants and stability constants with  $\text{Cu}^{2+}$ ,  $\text{Zn}^{2+}$ ,  $\text{Ca}^{2+}$ ,  $\text{Mg}^{2+}$  and  $\text{Na}^+$  ions are presented. The crystal structures of three ligands and one  $\text{Cu}^{2+}$  complex have also been determined by single-crystal X-ray diffraction analysis.

## Results and Discussion

### Acid–Base Properties

Phosphonic acids undergo their first deprotonation in the strongly acidic ( $\text{p}K_1 \leq 2$ ) and the second one in the weakly acidic region ( $\text{p}K_2 = 5\text{--}6$ ).<sup>[16]</sup> A different situation occurs in the case of bis(phosphonates), where a strong electrostatic interaction between the two geminal phosphonic acid groups results in a large enhancement of the basicity of the moiety. Furthermore, the presence of an amino group brings another protonation site into the molecule, which

affects the other protonation constants. The highest dissociation constants were determined by NMR titration following the procedure described recently in the literature.<sup>[17]</sup>

The ligands **H<sub>4</sub>pam**, **H<sub>4</sub>ale**, **H<sub>4</sub>meth** and **H<sub>4</sub>prop** exhibit similar acid–base behaviour, with five protonation constants spread over the whole pH range (Table 2). The first two  $\text{p}K_a$ 's lie in the strongly acidic region and correspond to the first deprotonation of each phosphonic acid group. The next constant is found close to the neutral region and represents release of the third proton from the bis(phosphonic acid) group, and the last two constants lie in the strongly alkaline region. The lower one is usually ascribed to the last deprotonation of the bis(phosphonic acid) moiety, and the last deprotonation occurs from the amino group.<sup>[18]</sup> The last proton is bound to the nitrogen atom in almost all poly(aminophosphonates).<sup>[19]</sup> This assignment can be supported by the crystal structure of the tris(ammonium) salt of **H<sub>4</sub>meth** (see below), whose structure contains a fully deprotonated bis(phosphonic acid) group, whereas the amino group remains protonated. The  $\text{p}K_a$  values of **H<sub>4</sub>meth** are somewhat distinct from those of the other ligands, with the most significant difference being observed for the  $\text{p}K_a(\text{HL}^{3-})$  and  $\text{p}K_a(\text{H}_2\text{L}^{2-})$  values, which are between one and two units lower than those found for the other ligands. Such behaviour can be explained by steric and/or electronic effects. The protonated amino group on the same carbon atoms can efficiently interact intramolecularly (electrostatically and/or through hydrogen bonds<sup>[20]</sup>) with only one negatively charged phosphonate group. The

Table 2. Values of protonation/dissociation constants of the ligands.

Species	H <sub>4</sub> pam		H <sub>4</sub> ale		H <sub>4</sub> meth		H <sub>4</sub> aca		H <sub>4</sub> prop	
	log $\beta$	pK <sub>a</sub>	log $\beta$	pK <sub>a</sub>	log $\beta$	pK <sub>a</sub>	log $\beta$	pK <sub>a</sub>	log $\beta$	pK <sub>a</sub>
HL <sup>3-</sup>	13.06(3) <sup>[a]</sup>	13.06	12.68(2) <sup>[a]</sup>	12.68	11.43(2)	11.43	10.73(4)	10.73	12.76(2) <sup>[a]</sup>	12.76
H <sub>2</sub> L <sup>2-</sup>	23.36(5)	10.30	23.75(1)	11.07	19.72(3)	8.29	18.22(6)	7.49	23.42(2)	10.66
H <sub>3</sub> L <sup>-</sup>	29.21(7)	5.85	30.11(1)	6.36	25.07(3)	5.35	23.98(7)	5.76	29.57(3)	6.15
H <sub>4</sub> L	31.01(9)	1.80	32.30(2)	2.19	26.25(6)	1.18	25.34(8)	1.36	31.68(4)	2.11
H <sub>5</sub> L <sup>+</sup>	–	<1.2	–	<1.2	–	<1.2	–	–	–	<1.2

[a] Determined by NMR titration. No control of the ionic strength.

other ligands with a more flexible carbon chain can be present in conformations where such convenient interaction(s) with both phosphonate groups are maximized. The strongest interaction should then be expected for H<sub>4</sub>pam, which contains the shortest ethylene chain, and, indeed, it exhibits the most basic last deprotonation. Alternatively, the presence of electron withdrawing (protonated) amino and phosphonic acid moieties on the same carbon atom ( $\alpha$  to each other) can decrease the values of all dissociation constants. A comparison of ligands H<sub>4</sub>pam and H<sub>4</sub>prop shows a small effect of the  $\alpha$ -hydroxo group on the acid–base properties of ligands.

The ligand H<sub>4</sub>aca contains an amide nitrogen atom instead of an amino group, which means that only four deprotonation steps can occur. The first one lies in the strongly acidic region, with two more in the neutral and the last one in the rather alkaline region. When compared with other bis(phosphonates) [e.g. methanediphosphonic acid: pK(HL<sup>3-</sup>) = 10.6, pK(H<sub>2</sub>L<sup>2-</sup>) = 7.05, pK(H<sub>3</sub>L<sup>-</sup>) = 2.77, pK(H<sub>4</sub>L) = 1.6],<sup>[21]</sup> H<sub>4</sub>aca shows higher overall basicity due to the higher value of pK(H<sub>3</sub>L<sup>-</sup>).

We carried out all measurements in the presence of non-complexing tetramethylammonium cations to avoid alkali metal ion complex formation, therefore our results differ from those reported in the literature (determined in the presence of Na<sup>+</sup> or K<sup>+</sup> ions).<sup>[5,6,9–13]</sup> The differences are particularly pronounced in the value of the last dissociation constant. In the presence of Na<sup>+</sup>/K<sup>+</sup> ions, the values reported in the literature are lower by one or even two orders of magnitude due to alkali metal ion assisted deprotonation (see Table S2 in the Supporting Information). Although the stabilities of the K<sup>+</sup> complexes of bis(phosphonates) are much lower than those with Na<sup>+</sup>, this interaction cannot be negligible<sup>[14,15]</sup> and the values of the dissociation/protonation constants should be changed.

## Complexation Properties

In order to simplify the following text we will use a three-digit code to describe the composition of the complexes. The first digit represents the number (stoichiometric coefficient) of protons, the second one is the number of ligand molecules and the third is the number of metal ions. A negative value of the first digit represents a hydroxo complex or untypical release of a proton(s) from, under common conditions, a fully deprotonated ligand molecule, for example alkoxide anion formation. As an example, a com-

plex with an [H<sub>2</sub>L<sub>2</sub>M] stoichiometry is referred to as [221] and the value of its overall stability constant as log  $\beta_{221}$ . The charges of the complexes are omitted, and throughout the following text pH means  $-\log[\text{H}^+]$ .

## Divalent Metal Ions

Speciation of the complexes with biogenic metal ions (Cu<sup>2+</sup>, Zn<sup>2+</sup>, Ca<sup>2+</sup> and Mg<sup>2+</sup>) in aqueous solution was studied by potentiometry (Figure 2). Following the procedure described in the Experimental Section, three sets of data with ligand-to-metal ratios 1:1, 2:1 and 1:2 were recorded for each ion. All these measurements were complicated by precipitate formation. In general, the precipitation started with increasing abundance of the uncharged [211] complex at a pH between 2.5 and 6.0. The precipitate was usually fully dissolved under basic conditions (pH 9–11, depending on the ligand and metal combination and ratio; see Table S1). Additionally, in some cases data could not be recorded due to extended precipitate formation over a wide pH range, especially for systems containing H<sub>4</sub>meth or for mixtures with an excess of metal ion. Obviously, the stability constants of the species abundant mostly in the pH range where the precipitates were present were not accessible, which means that a chemical model for many systems does not involve non-protonated species and direct comparison of the complexation properties of different ligands is somewhat difficult. The results are compiled in Table 3, and all distribution diagrams are provided as Supporting Information (Figures S2–S7).

The chemical models for speciation of H<sub>4</sub>pam, H<sub>4</sub>ale, H<sub>4</sub>meth and H<sub>4</sub>prop complexes are similar. Complexation starts below pH 2 with formation of the [311] complex. At higher pH, less protonated species are present. The high negative charge of the fully deprotonated bis(phosphonate) group of the ligands disfavours formation of the [021] complexes and only the [121] and [221] species can be found in mixtures with an excess of the ligands. From a comparison of the constants corresponding to coordination of the first and second ligand molecules in their monoprotonated form (i.e. formation of the [111] and [221] complexes; Table 4), it is clear that the second consecutive stability constants are only slightly lower than the first ones. This fact indicates negligible steric crowding due to coordination of the first protonated ligand molecule.

In equimolar solutions and at metal excess, 1:2 L:M complexes are formed under neutral and alkaline conditions. As one ligand molecule binds two metal ions, all the protons

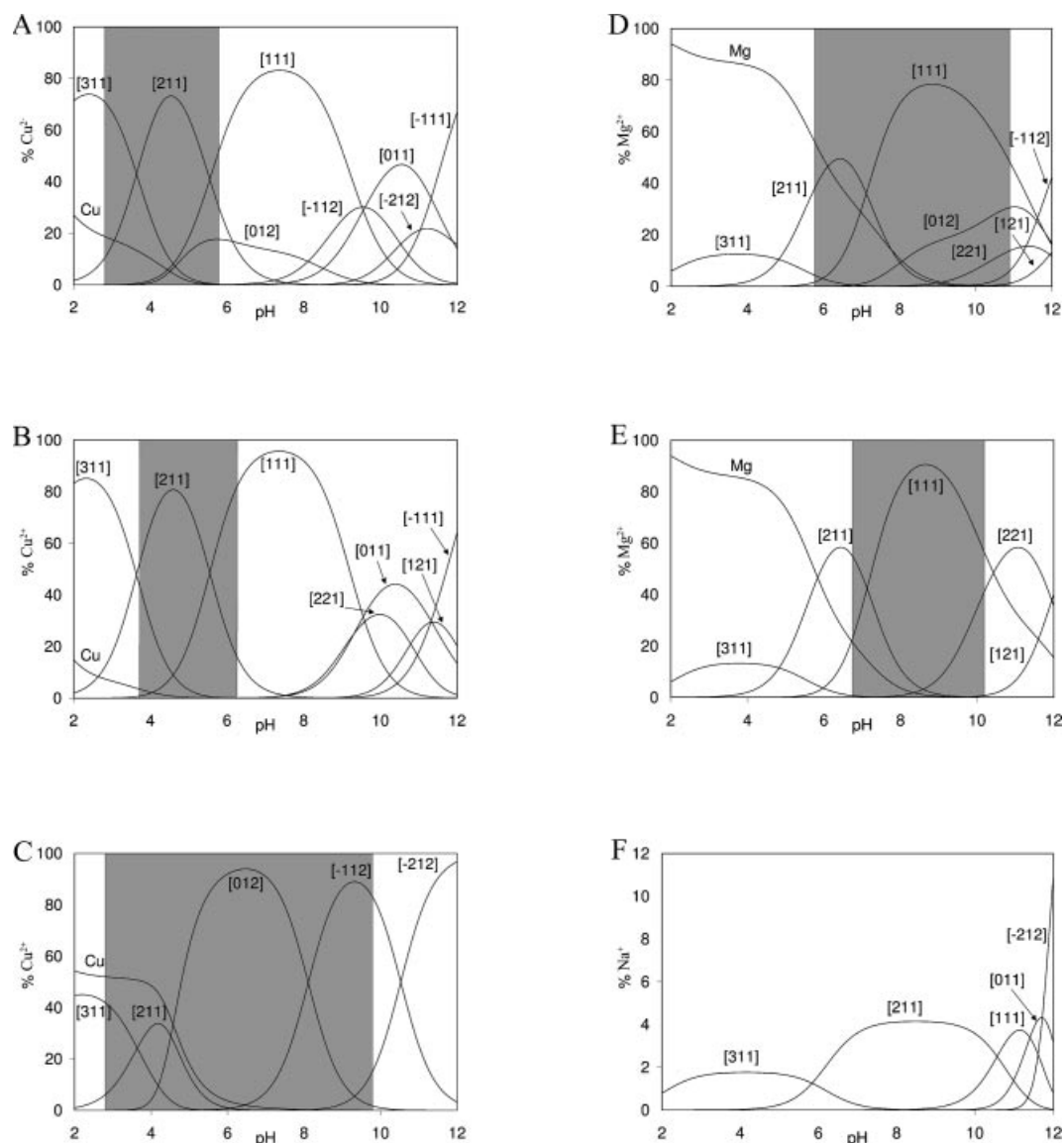


Figure 2. Species distribution plot for aqueous solutions of Cu<sup>2+</sup> and H<sub>4</sub>ale with metal/ligand ratios of 1:1 (A), 1:2 (B) and 2:1 (C); Mg<sup>2+</sup> and H<sub>4</sub>ale 1:1 (D) and 1:2 (E); Na<sup>+</sup> and H<sub>4</sub>ale 10:1 (F). The grey areas were not studied during the experiment due to formation of a precipitate.

are released and these complexes do not exist in a protonated form. All systems containing Cu<sup>2+</sup> and Zn<sup>2+</sup> exhibit a high abundance of the [-111], [-112] and [-212] species in the alkaline region. In these complexes, deprotonation of the coordinated water molecule and/or deprotonation of the hydroxy group of ligands H<sub>4</sub>pam and H<sub>4</sub>ale has to occur, although these two possibilities could not be distinguished by potentiometry due to a proton ambiguity. As expected, the stability of the complexes follows the order Cu<sup>2+</sup> > Zn<sup>2+</sup> > Mg<sup>2+</sup> > Ca<sup>2+</sup>. The stabilities of the complexes with H<sub>4</sub>pam, H<sub>4</sub>ale and H<sub>4</sub>prop are similar, whereas the presence of an amino group in the  $\alpha$  position decreases the basicity of H<sub>4</sub>meth and leads to a lower stability of its complexes.

As H<sub>4</sub>aca contains an amide group instead of an amino group it prefers to form less protonated complexes and the complexation process starts at higher pH. The same effect was observed for 2:1 L:M complexes, where the [021] com-

plex was found in all systems containing H<sub>4</sub>aca. The stability constants of H<sub>4</sub>aca complexes are between the values found for H<sub>4</sub>meth and those found for the other ligands. In conclusion, the stabilities of the complexes follow the general order H<sub>4</sub>pam  $\approx$  H<sub>4</sub>ale  $\approx$  H<sub>4</sub>prop > H<sub>4</sub>aca > H<sub>4</sub>meth.

The solid-state structures of bis(phosphonate) complexes typically show oligomeric or polymeric coordination chains with the bis(phosphonic acid) group acting as a bridging moiety.<sup>[22]</sup> Therefore, the presence of these complicated structures in solution is expected as well.<sup>[18]</sup> Unfortunately, the complexity of the studied systems did not allow us to take these multinuclear/polymeric complexes into account during the refinement of the potentiometric data.

### Sodium

As expected, the complexes with Na<sup>+</sup> ion exhibit the lowest stability constants of all the metal ions studied (Table 3),

Table 3. Stability constants of metal–ligand complexes.

Cation	<i>h</i>	<i>l</i>	<i>m</i>	H <sub>4</sub> pam	H <sub>4</sub> ale	log $\beta_{hlm}$ H <sub>4</sub> meth	H <sub>4</sub> aca	H <sub>4</sub> prop
Cu <sup>2+</sup>	3	1	1	32.66(8)	33.82(3)	[a]	–	32.90(3)
	2	1	1	29.53(6)	30.20(3)	[a]	23.95(1)	29.30(3)
	1	1	1	–	24.65(4)	[a]	19.40(3)	–
	0	1	1	–	15.09(6)	[a]	13.71(6)	–
	–1	1	1	5.30(9)	3.78(5)	[a]	2.98(6)	3.14(6)
	2	2	1	42.4(1)	41.69(8)	[a]	–	41.44(8)
	1	2	1	–	30.90(7)	[a]	29.02(8)	30.60(8)
	0	2	1	–	–	[a]	18.6(1)	–
	0	1	2	–	23.4(1)	[a]	–	24.63(4)
	–1	1	2	18.6(2)	15.31(8)	[a]	–	14.76(8)
Zn <sup>2+</sup>	–2	1	2	–	4.76(8)	[a]	2.60(7)	4.13(6)
	3	1	1	31.48(4)	32.52(2)	–	26.74(9)	31.75(2)
	2	1	1	28.24(3)	28.85(3)	23.54(7)	23.72(6)	–
	1	1	1	–	22.68(7)	–	–	24.36(6)
	0	1	1	11.57(6)	12.5(1)	–	9.8(1)	14.78(7)
	–1	1	1	1.12(8)	1.23(8)	–1.34(1)	–0.79(8)	3.91(7)
	2	2	1	39.10(8)	40.43(8)	32.17(3)	–	44.9(1)
	1	2	1	–	29.30(9)	22.46(7)	–	33.9(1)
	0	2	1	–	–	–	13.44(8)	22.7(1)
	–1	1	2	9.0(2)	–	5.83(4)	–	–
Ca <sup>2+</sup>	–2	1	2	–	–0.77(8)	–	–2.64(6)	–
	2	1	1	[a]	26.70(8)	[a]	[a]	25.82(2)
	1	1	1	[a]	17.25(8)	[a]	[a]	15.72(8)
	1	2	1	[a]	20.8(1)	[a]	[a]	20.00(6)
Mg <sup>2+</sup>	0	1	2	[a]	9.1(1)	[a]	[a]	–
	3	1	1	30.6(2)	31.56(6)	–	–	30.78(9)
	2	1	1	26.68(3)	26.89(2)	–	–	26.29(2)
	1	1	1	20.08(7)	19.78(5)	18.2(4)	19.79(3)	18.80(4)
	0	1	1	–	–	7.7(4)	9.32(5)	–
	2	2	1	37.3(2)	36.19(9)	32.6(4)	–	–
	1	2	1	25.8(1)	24.24(8)	21.6(4)	–	–
	0	2	1	–	–	–	12.54(9)	–
	0	1	2	15.2(2)	13.9(1)	–	–	14.86(2)
	–1	1	2	–	2.3(1)	–	–	–
Na <sup>+</sup>	3	1	1	29.5(1)	30.73(6)	25.8(1)	–	30.31(8)
	2	1	1	24.23(6)	24.98(3)	20.6(1)	19.54(8)	24.46(7)
	1	1	1	14.82(3)	14.43(3)	12.83(5)	12.36(7)	14.53(4)
	0	1	1	3.25(2)	3.04(2)	1.74(4)	2.04(5)	–
	–1	1	2	–	–	–9.51(6)	–8.52(4)	–7.20(2)
	–2	1	2	–19.22(2)	–19.26(2)	–	–	–

[a] These systems were not studied due to extensive precipitate formation.

Table 4. Formation constants of the [111] and [221] complexes.

	Cu <sup>2+</sup> :H <sub>4</sub> ale	Zn <sup>2+</sup> :H <sub>4</sub> ale	Zn <sup>2+</sup> :H <sub>4</sub> prop	Mg <sup>2+</sup> :H <sub>4</sub> pam	Mg <sup>2+</sup> :H <sub>4</sub> ale	Mg <sup>2+</sup> :H <sub>4</sub> meth
M + HL $\rightleftharpoons$ MHL	24.7	22.7	24.4	20.1	19.8	18.2
MHL + HL $\rightleftharpoons$ M(HL) <sub>2</sub>	17.0	17.8	20.5	17.2	16.4	14.4

therefore a 1:10 L:M ratio was used to obtain a reasonable abundance of the complexes in solution. No precipitation was observed in these systems. For H<sub>4</sub>pam, H<sub>4</sub>ale, H<sub>4</sub>meth and H<sub>4</sub>prop, interaction starts below pH 2 with formation of the [311] complex. H<sub>4</sub>aca exhibits similar differences to those described above (complexation starts at higher pH (3–4) with formation of the [211] complex). Despite a tenfold excess of Na<sup>+</sup> ions, less than 60% of the ligand is present in the form of complexes below pH 10, where only 1:1 L:M complexes are present. Under strongly alkaline conditions, the 1:2 L:M hydroxo species are present in significant abun-

dance. Formation of the [–112] and [–212] species can be explained by deprotonation of the water molecules coordinated to the Na<sup>+</sup> ion and/or deprotonation of  $\alpha$ -hydroxo group. Although formation of the Na<sup>+</sup> hydroxo complexes is unusual, their inclusion in the calculations significantly improves the fit of the experimental data (Figure S1). The presence of a hydroxide anion in the solid-state structure of trisodium phosphate is well known.<sup>[23,24]</sup> The stability order of the complexes is the same as that found for the divalent metal ions (H<sub>4</sub>pam  $\approx$  H<sub>4</sub>ale  $\approx$  H<sub>4</sub>prop > H<sub>4</sub>aca > H<sub>4</sub>meth).



## Simulation of Speciation under Physiological Conditions

At physiological pH, all studied aminoalkylbis(phosphonates) are present mostly in their doubly protonated form ( $\text{H}_2\text{L}$ )<sup>2+</sup>. As the third dissociation constant of the amide derivative  $\text{H}_4\text{aca}$  is 7.49, both ( $\text{Haca}$ )<sup>2+</sup> and ( $\text{H}_2\text{aca}$ )<sup>+</sup> are present in almost equimolar concentrations at a pH of around 7. As strongly acidic conditions are necessary for protonation of bis(phosphonates) to form  $\text{H}_4\text{L}$  species, these compounds remain in the ionised form in living organisms, thus disfavoured their absorption in the gastrointestinal tract upon oral administration.<sup>[1]</sup>

To demonstrate the speciation of aminoalkylbis(phosphonates) in body liquids, we chose the commercially applied ligand Aledronate ( $\text{H}_4\text{ale}$ ). With the concentrations of metal ions commonly found in human blood plasma ( $\text{Cu}^{2+}$ : 0.15  $\mu\text{M}$ ;  $\text{Zn}^{2+}$ : 0.2  $\mu\text{M}$ ;  $\text{Ca}^{2+}$ : 3 mM;  $\text{Mg}^{2+}$ : 1 mM;  $\text{Na}^+$ : 0.138 M)<sup>[25]</sup> and at physiological pH (7.4), we obtained the abundances shown in Figure 3. It is evident that the majority of the ligand (approx. 90%) is bound in the form of  $\text{Ca}^{2+}$ ,  $\text{Mg}^{2+}$  and  $\text{Na}^+$  complexes. The complexes are uncharged or singly negatively charged. As the form (free acid/complex, charge, polarity etc.) could dramatically change the pharmacological behaviour of the studied compound, formation of the above-mentioned complexes should be carefully taken into account during all medical and biological studies dealing with bis(phosphonates). Whereas alkali and alkaline earth metal complexes are preferentially formed due to high concentration of these metal ions at higher Aledronate concentrations, at lower Aledronate concentrations (<10<sup>-5</sup> M) the high stabilities of the transition metal complexes become important and increasing abundances of  $\text{Cu}^{2+}$  and  $\text{Zn}^{2+}$  complexes are obtained. The high stability of these complexes could decrease the bioavailability of the bis(phosphonate). In real living systems, we should expect a slightly lower abundance of these complexes due to the presence of many natural ligands (acetate, citrate, amino acids, phosphates etc.) that compete with bis-

(phosphonate) ligands. The effect of bioligands on the abundance of complexes with alkali and alkaline earth metal ions is probably negligible due to the low stability of the complexes with these bioligands.

## Crystal Structures

The crystal structures of  $\text{H}_4\text{meth}$ ,  $\text{H}_4\text{aca}$  and  $\text{H}_4\text{prop}$  with various degrees of protonation and the  $\text{Cu}^{2+}$  complex of  $\text{H}_4\text{pam}$  were determined.

The phosphonate groups in the structure of  $\text{H}_4\text{aca}\cdot\text{thf}$  are fully protonated (Figure 4). A lower hydrophilicity of the amide-containing ligand results in the formation of a solvate with one molecule of thf and two layers in the crystal. One layer consists of the ligand molecules, which are connected to each other by hydrogen bonds, and the second one is formed by thf molecules (Figure 5, Table S3). The

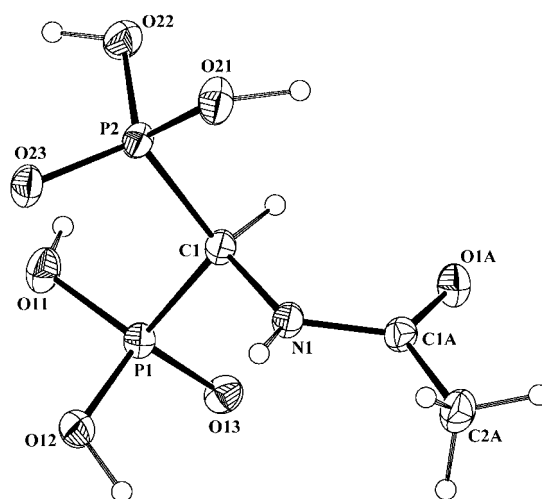


Figure 4. The molecular structure of  $\text{H}_4\text{aca}$  in the crystal structure of  $\text{H}_4\text{aca}\cdot\text{thf}$ .

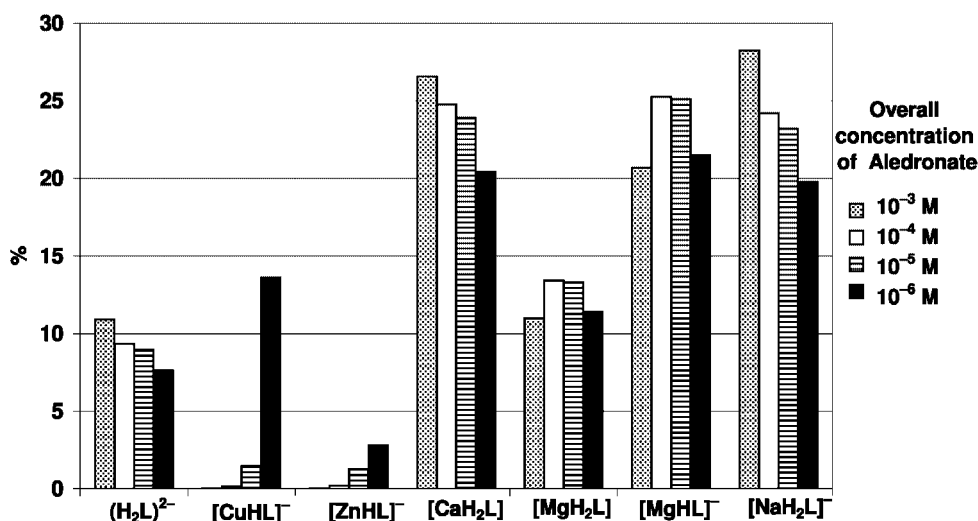


Figure 3. Simulation of the distribution of Aledronate ( $\text{H}_4\text{ale}$ )-containing species in human blood plasma.

position of the thf molecules is stabilized by hydrogen bonds between the ether oxygen atom and the phosphonate hydroxo groups of the ligand. The geometry around the phosphorus atoms is roughly tetrahedral, with slightly longer P–O distances to the protonated oxygen atoms than to the phosphoryl oxygen atom (Table 5).

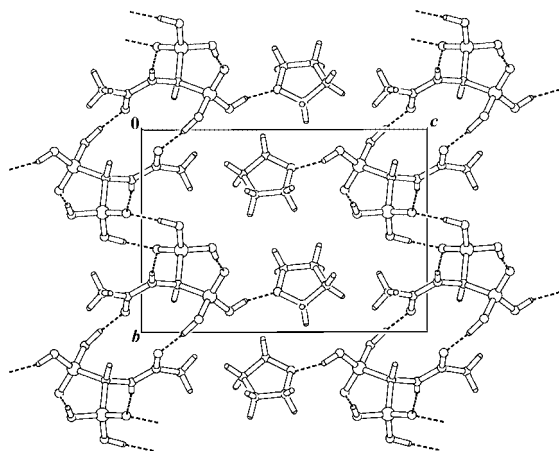


Figure 5. Crystal packing in the structure of  $H_4aca \cdot thf$ .

Table 5. Geometry around the phosphorus atoms in the crystal structures of the free ligands.

	$H_4aca \cdot thf$	$(NH_4)(H_3prop) \cdot H_2O$	$(NH_4)_3(Hmeth) \cdot H_2O$
P1–O11	1.528(1)	1.572(1)	1.519(1)
P1–O12	1.551(1)	1.510(1)	1.529(1)
P1–O13	1.495(1)	1.514(1)	1.522(1)
P1–C1	1.825(2)	1.812(2)	1.842(1)
P2–O21	1.537(2)	1.580(1)	1.520(1)
P2–O22	1.542(2)	1.500(1)	1.524(1)
P2–O23	1.484(1)	1.514(1)	1.517(1)
P2–C1	1.826(2)	1.827(2)	1.839(1)
C1–P1–O11	108.6(1)	106.6(1)	107.0(1)
C1–P1–O12	106.3(1)	109.4(1)	103.5(1)
C1–P1–O13	107.5(1)	107.0(1)	109.0(1)
O11–P1–O12	113.2(1)	108.0(1)	112.2(1)
O11–P1–O13	115.9(1)	109.6(1)	112.0(1)
O12–P1–O13	104.9(1)	115.9(1)	112.5(1)
C1–P2–O21	105.8(1)	104.4(1)	105.8(1)
C1–P2–O22	104.6(1)	108.1(1)	107.4(1)
C1–P2–O23	112.7(1)	111.0(1)	103.8(1)
O21–P2–O22	108.7(1)	109.6(1)	113.3(1)
O21–P2–O23	111.7(1)	109.4(1)	113.1(1)
O22–P2–O23	112.8(1)	113.9(1)	112.6(1)

A lower degree of protonation was found in  $(NH_4)(H_3prop) \cdot H_2O$  (Figure 6). Each phosphonic acid group and the amino group binds one proton. The P–O bonds are noticeably longer to the protonated oxygen atoms, and the geometry around the phosphorus atoms is tetrahedral (Table 5). The crystal structure is stabilized by an extensive three-dimensional framework of hydrogen bonds between the phosphonate oxygen atoms, the ligand amino group, the ammonia cations and co-crystallised water molecule (Table S4).

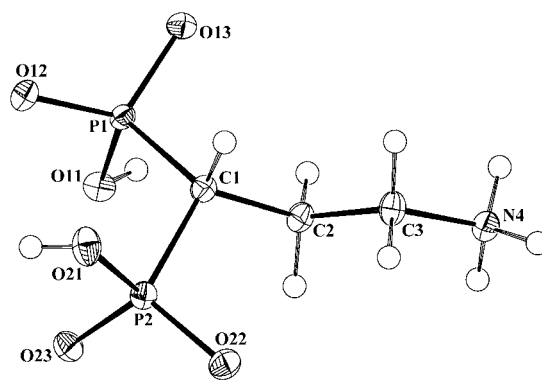


Figure 6. The molecular structure of  $H_3prop^-$  in the crystal structure of  $(NH_4)(H_3prop) \cdot H_2O$ .

The bis(phosphonic acid) group in the single crystals of  $(NH_4)_3(Hmeth) \cdot H_2O$  is fully deprotonated (Figure 7). The negative charge of the bis(phosphonic) unit is compensated by three ammonium cations and the protonated amino group of the ligand molecule. All phosphonate oxygen atoms are equivalent due to charge delocalisation (Table 5). An extended hydrogen-bond framework is also found in this structure. The ammonia cations are bound to phosphonate oxygen atoms by strong hydrogen bonds (O–N distances in the range 2.68–3.01 Å, Table S5). In addition, the co-crystallised water molecule forms hydrogen bonds with the phosphonate oxygen atoms (Ow–O distances of 2.77 and 2.90 Å, Table S5). This is the first reported structure to directly confirm the expected protonation scheme of aminoalkylbis(phosphonates). As the last proton is localised on the amino group, this supports the assumption that the final dissociation constant corresponds to a release of the proton from this group.

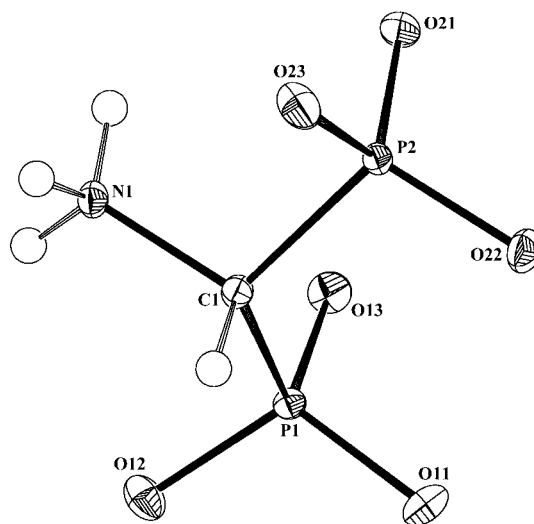


Figure 7. Molecular structure of  $(Hmeth)^{3-}$  in the crystal structure of  $(NH_4)_3(Hmeth) \cdot H_2O$ .

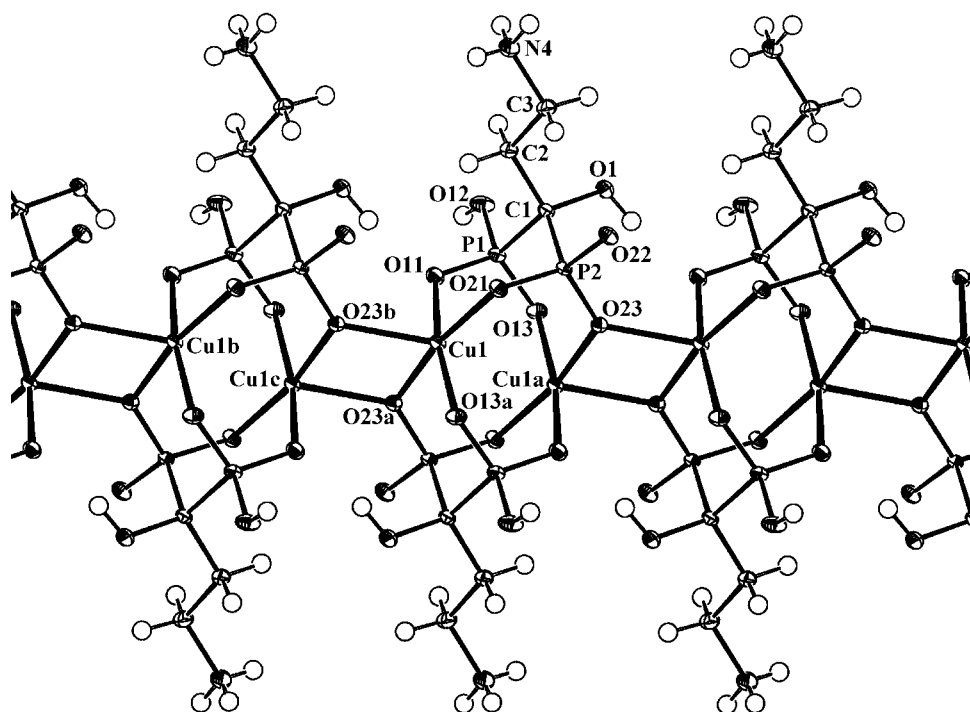


Figure 8. Chain design of  $[\text{Cu}_2(\text{H}_2\text{pam})_2]_n$  from the crystal structure of the  $[\{\text{Cu}_2(\text{H}_2\text{pam})_2\} \cdot \text{H}_2\text{O}]_n$ . Symmetry operations: a:  $-x + 2, -y + 1, -z + 1$ ; b:  $x - 1, y, z$ ; c:  $-x + 1, -y + 1, -z + 1$ .

The crystal structure of  $[\{\text{Cu}_2(\text{H}_2\text{pam})_2\} \cdot \text{H}_2\text{O}]_n$  shows an infinite linear polymeric chain. The coordination sphere of the  $\text{Cu}^{2+}$  ion is square-pyramidal (Figure 8, Table 6). The basal plane of the pyramid is formed by one oxygen atom of each phosphonic acid group of two different ligand molecules (O11, O21, O13a and O23a), and one of the oxygen atoms of the basal plane of the neighbouring unit is coordinated to the  $\text{Cu}^{2+}$  ion in the apical position (O23b)

to form a four-membered metallacycle with a Cu1–Cu1c separation of 3.21 Å. Each tetragonal pyramid is linked by a bridging ligand to a neighbouring molecule lying below the basal plane, with a Cu1–Cu1a separation of 2.99 Å. The geometrical parameter  $\tau$  has a value of 0.005, which corresponds to an almost ideal square pyramid (theoretical value of  $\tau = 0$ , compared to an ideal trigonal bipyramid with  $\tau = 1$ ).<sup>[26]</sup> One uncoordinated phosphonate oxygen atom is protonated as well as an amino group, and the coordination polymeric chains are connected by hydrogen bonds (Table S6).

The Cu1–Cu1a distance of 2.99 Å in the  $\text{Cu}_2(\text{pam})_2$  moiety is too long for metal–metal bond formation. A similar design was previously found for  $\text{Cu}^{2+}$  complexes of 1-hydroxyethyl-1,1-bis(phosphonic acid),<sup>[27]</sup> with protonated diaminoalkanes as counter cations. These compounds show a moderately strong antiferromagnetic interaction.<sup>[27,28]</sup>

## Conclusions

We have reported the acid–base and complexation behaviour of five bis(phosphonate) ligands containing an amino group in the side chain. The protonation constants and stability constants of their complexes with  $\text{Cu}^{2+}$ ,  $\text{Zn}^{2+}$ ,  $\text{Ca}^{2+}$ ,  $\text{Mg}^{2+}$  and  $\text{Na}^+$  ions have been determined by means of potentiometric titrations. The bis(phosphonic acid) group exhibits four dissociation constants — two in the strongly acidic region, the third in the neutral region and the last one in the alkaline region. The amino groups undergo deprotonation under strongly alkaline conditions. Determi-

Table 6. Bond lengths and angles found in the structure of  $[\{\text{Cu}_2(\text{H}_2\text{pam})_2\} \cdot \text{H}_2\text{O}]_n$ .<sup>[a]</sup>

P1–O11	1.530(1)	Cu1–O13a	1.953(1)
P1–O12	1.539(2)	Cu1–O11	1.966(1)
P1–O13	1.522(2)	Cu1–O21	1.986(1)
P1–C1	1.838(2)	Cu1–O23a	2.011(1)
P2–O21	1.532(1)	Cu1–O23b	2.191(1)
P2–O22	1.520(1)		
P2–O23	1.534(1)		
P2–C1	1.852(2)		
C1–P1–O11	107.1(1)	O13a–Cu1–O11	167.0(1)
C1–P1–O12	104.1(1)	O13a–Cu1–O21	90.1(1)
C1–P1–O13	108.4(1)	O13a–Cu1–O23a	89.0(1)
O11–P1–O12	111.2(1)	O13a–Cu1–O23b	100.7(1)
O11–P1–O13	113.6(1)	O11–Cu1–O21	90.5(1)
O12–P1–O13	111.9(1)	O11–Cu1–O23a	87.7(1)
C1–P2–O21	106.2(1)	O11–Cu1–O23b	91.1(1)
C1–P2–O22	109.0(1)	O21–Cu1–O23a	167.4(1)
C1–P2–O23	104.6(1)	O21–Cu1–O23b	112.2(1)
O21–P2–O22	113.4(1)	O23a–Cu1–O23b	80.4(1)
O21–P2–O23	112.8(1)		
O22–P2–O23	110.4(1)		

[a] Symmetry operations: a:  $-x + 2, -y + 1, -z + 1$ ; b:  $x - 1, y, z$ ; c:  $-x + 1, -y + 1, -z + 1$ .



nation of the stability constants was complicated by the precipitation of insoluble complexes. The stability constants of the complexes follow the order  $H_4pam \approx H_4ale \approx H_4prop > H_4aca > H_4meth$ . Complicated chemical models containing complexes with 1:1, 2:1 and 1:2 L:M ratios and various degrees of protonation were found for all systems with divalent metals. In  $Na^+$ -containing systems, 1:1 complexes cover the whole pH scale except strongly alkaline conditions, where 2:1 complexes are present. A comparison of the properties of the studied ligands has shown a negligible effect of the  $\alpha$ -hydroxy group on the acid–base and coordination properties of the bis(phosphonates), whereas the presence of the amino group in the  $\alpha$  position significantly decreases the overall basicity of the ligand and the stability of its complexes. Simulation of Aledronate ( $H_4ale$ ) speciation in human blood plasma shows a high abundance of  $Ca^{2+}$ ,  $Mg^{2+}$  and  $Na^+$  complexes. At lower overall concentrations of bis(phosphonate), increasing abundances of  $Cu^{2+}$  and  $Zn^{2+}$  complexes are expected. The crystal structures of the ligands show a different degree of protonation. The structure of the triammonium salt of aminomethylbis(phosphonic acid), which contains a monoprotonated ligand molecule, nicely documents the protonation scheme of the studied compounds — the last proton is released from the amino group. The crystal structure of the  $Cu^{2+}$  complex of  $H_4pam$  shows a polymeric coordination chain. The square-pyramidal coordination sphere of  $Cu^{2+}$  contains five oxygen atoms from five different phosphonic acid groups. In the polymeric chain, two tetragonal pyramids are oriented towards each other and their basal planes are linked together with a Cu–Cu distance of 2.99 Å.

## Experimental Section

**Materials and Methods:** Commercially available chemicals were of synthetic purity and were used as received. Acetonitrile was dried by distillation from  $P_2O_5$ . Elemental analyses were performed at the Institute of Macromolecular Chemistry (Academy of Science of the Czech Republic, Prague).  $^1H$  (400 MHz) and  $^{31}P$  (161.9 MHz) NMR spectra were recorded with a Varian UNITY PLUS-400 spectrometer in 5-mm sample tubes. NMR experiments were performed at 298 K. For the measurements in  $D_2O$ , *tert*-butyl alcohol was used as an internal standard with the methyl signal referenced to  $\delta = 1.20$  ppm ( $^1H$ ). For the measurements in  $CDCl_3$ , tetramethylsilane was used as an internal standard with the methyl signal referenced to  $\delta = 0.00$  ppm ( $^1H$ ). The  $^{31}P$  chemical shifts were measured with respect to 1%  $H_3PO_4$  in  $D_2O$  as an external standard (substitution method). Mass spectra were recorded with a Bruker Esquire 3000 spectrometer equipped with an electrospray ion source and an ion trap detector. All measurements were carried out in the positive-ion mode.

**Synthesis:** Ligands  $H_4pam$ ,<sup>[29]</sup>  $H_4ale$ ,<sup>[29]</sup>  $H_4meth$ <sup>[30]</sup> and  $H_4prop$ <sup>[31]</sup> were prepared by modification of reported procedures. The ligands were chemically pure (NMR, MS) and composition of the samples was checked by elemental analysis; see the Supporting Information for full experimental and analytical details, and discussion of the synthesis.

**Tetraethyl Acetamidomethylbis(phosphonate):** A solution of tetraethyl aminomethylbis(phosphonate)<sup>[30]</sup> (4.0 g, 13.2 mmol) in dry

acetonitrile (50 mL) was added dropwise to a solution of acetyl chloride (3.0 g, 38.2 mmol) and  $Na_2CO_3$  (5.2 g, 49 mmol) in dry acetonitrile (50 mL) at  $-40^\circ C$ . After the addition was finished, the mixture was warmed slowly to room temperature and stirred overnight. After treatment with charcoal and filtration, the unreacted acetyl chloride was removed by repeated vacuum evaporation with toluene. The product was obtained as a colourless oil in a yield of 4.4 g (97%).  $C_7H_{17}NO_8P_2$ : calcd. C 29.28, H 5.27, N 4.88; found C 29.42, H 5.41, N 4.25.  $^1H$  NMR ( $CDCl_3$ ):  $\delta = 1.34$  (m, 12 H,  $CH_2CH_3$ ), 2.08 (s, 3 H,  $CH_3CO$ ), 4.19 (m, 8 H,  $OCH_2$ ), 5.06 (td,  $^2J_{PH} = 21.4$ ,  $^3J_{HH} = 10.4$  Hz, 1 H, *PCHP*), 6.75 (br. s, 1 H, *NH*) ppm.  $^{31}P$  NMR ( $CDCl_3$ ):  $\delta = 17.0$  ppm (d,  $^2J_{H,P} = 21.4$  Hz). ESI/MS: calculated 368.3; found 368.3 [ $M + Na^+$ ].

**Acetamidomethylbis(phosphonic acid) ( $H_4aca$ ):** Tetraethyl acetamidomethylbis(phosphonate) (3.0 g, 8.7 mmol) was dissolved in 30%  $HBr/AcOH$  (50 mL) in a 100-mL flask and stirred for 24 h at room temperature. After removal of the volatiles on a rotary evaporator, the resulting oil was dissolved in EtOH (30 mL). Precipitation of the crude product from solution occurred on standing. After 3 h, the precipitate was filtered off and extracted with boiling EtOH (100 mL). After filtration with charcoal, volatiles were removed in vacuo. The crude product was recrystallised from water by addition of thf. The product was filtered, washed with thf and dried at room temperature over  $P_2O_5$ . Yield: 1.7 g (63%) as adduct **6**·thf.  $C_7H_{17}NO_8P_2$ : calcd. C 27.55, H 5.61, N 4.59; found C 27.62, H 5.60, N 4.35.  $^1H$  NMR ( $D_2O/NaOD$ ):  $\delta = 1.63$  (m, 4 H,  $CH_2CH_2CH_2$  thf),  $\delta = 1.94$  (s, 3 H,  $CH_3CO$ ),  $\delta = 3.49$  (m, 4 H,  $CH_2CH_2O$  thf), 4.46 (t,  $^2J_{PH} = 21.3$  Hz, 1 H, *PCHP*) ppm.  $^{31}P$  NMR ( $D_2O/NaOD$ ):  $\delta = 17.0$  ppm (d,  $^2J_{H,P} = 21.3$  Hz). ESI/MS: calculated 256.0; found 255.8 [ $M + Na^+$ ].

**Crystal-Structure Determination:** Single crystals of  $H_4aca$ ·thf were selected from the recrystallised matter before the filtration. Single crystals of  $(NH_4)(H_3prop) \cdot H_2O$  were prepared by the following method:  $H_4prop$  was dissolved in concentrated ammonia, the solution was evaporated, and the oily residue was dissolved in water and crystallised by slow vapour diffusion of *i*PrOH into the solution. Single crystals of  $(NH_4)_3(Hmeth) \cdot H_2O$  were prepared by slow vapour diffusion of EtOH into a solution of  $H_4meth$  in 5% ammonia. Single crystals of  $[Cu_2(H_2pam)_2] \cdot H_2O$  were prepared by hydrothermal synthesis. Thus,  $H_4pam$  (352.5 mg, 1.50 mmol) and  $CuCO_3$  (185.1 mg, 1.50 mmol) were suspended in water (30 mL) and the mixture was heated at  $70^\circ C$  in a closed flask. After three weeks, shiny greenish-blue needles of  $[Cu_2(H_2pam)_2] \cdot H_2O$  had formed. They were decanted off and dried in air. Yield: 446.3 mg (95%).  $C_6H_{20}Cu_2N_2O_{15}P_4$ : calcd. C 20.79, H 3.30, N 4.58; found C 21.05, H 3.48, N 4.39.

The selected crystals were mounted on glass fibres in a random orientation in silicone grease or epoxide glue. Diffraction data were collected using graphite-monochromated Mo- $K_\alpha$  radiation with an Enraf–Nonius KappaCCD diffractometer at 150(1) K [Cryostream Cooler (Oxford Cryosystem)] or 294(1) K and analysed using the HKL DENZO program package.<sup>[32]</sup> The structures were solved by direct methods, and refined by full-matrix least-squares techniques (SIR92,<sup>[33]</sup> SHELXL97<sup>[34]</sup>). The scattering factors used for neutral atoms were included in the SHELXL97 program. In the case of  $[Cu_2(H_2pam)_2] \cdot H_2O$ , a Gaussian absorption correction was applied.<sup>[35]</sup> Further details are given in Table 7.

All non-hydrogen atoms were refined anisotropically. In the structure of  $H_4aca$ ·thf, the molecule of tetrahydrofuran solvate was found to be very disordered. This disorder was refined by splitting the carbon chain into two positions with occupancies of 61:39. The hydrogen atoms of the ligand molecule were localised in the electronic density difference map, however, they were fixed in theoretic

Table 7. Experimental data of reported crystal structures.

	H <sub>4</sub> aca·thf	(NH <sub>4</sub> )(H <sub>3</sub> prop)·H <sub>2</sub> O	(NH <sub>4</sub> ) <sub>3</sub> (Hmeth)·H <sub>2</sub> O	{[Cu <sub>2</sub> (H <sub>2</sub> pam) <sub>2</sub> ]·H <sub>2</sub> O} <sub>n</sub>
Formula	C <sub>7</sub> H <sub>17</sub> NO <sub>8</sub> P <sub>2</sub>	C <sub>3</sub> H <sub>16</sub> N <sub>2</sub> O <sub>7</sub> P <sub>2</sub>	CH <sub>18</sub> N <sub>4</sub> O <sub>7</sub> P <sub>2</sub>	C <sub>3</sub> H <sub>11</sub> CuNO <sub>8</sub> P <sub>2</sub>
Molecular wt.	305.16	254.12	260.13	314.61
Colour	colourless	colourless	colourless	greenish blue
Shape	rod	plate	prism	rod
Dimensions [mm]	0.10 × 0.25 × 0.50	0.03 × 0.20 × 0.28	0.33 × 0.40 × 0.50	0.13 × 0.15 × 0.40
Crystal system	triclinic	monoclinic	orthorhombic	monoclinic
Space group	<i>P</i> 1̄ (no. 2)	<i>C</i> 2/ <i>c</i> (no. 15)	<i>Pna</i> 2 <sub>1</sub> (no. 62)	<i>P</i> 2 <sub>1</sub> / <i>c</i> (no. 14)
<i>a</i> [Å]	5.2717(2)	13.0593(3)	17.9266(1)	5.4824(1)
<i>b</i> [Å]	9.5220(3)	7.2487(2)	9.6087(2)	14.3335(4)
<i>c</i> [Å]	13.1921(5)	21.3368(5)	6.2007(4)	11.6411(3)
<i>α</i> [°]	89.261(2)	90	90	90
<i>β</i> [°]	85.688(2)	100.0962(15)	90	103.1868(15)
<i>γ</i> [°]	76.917(3)	90	90	90
<i>V</i> [Å <sup>3</sup> ]	643.19(4)	1988.53(9)	1068.08(7)	890.66(4)
<i>Z</i>	2	8	4	4
<i>D<sub>c</sub></i> [g cm <sup>-3</sup> ]	1.576	1.698	1.618	2.346
<i>T</i> [K]	294(1)	150(1)	150(1)	150(1)
<i>θ</i> range [°]	3.10–27.50	1.94–27.48	2.40–27.49	3.36–27.48
Index ranges	−6 ≤ <i>h</i> ≤ 6 −11 ≤ <i>k</i> ≤ 12 −17 ≤ <i>l</i> ≤ 17	−16 ≤ <i>h</i> ≤ 16 −9 ≤ <i>k</i> ≤ 9 −27 ≤ <i>l</i> ≤ 27	−23 ≤ <i>h</i> ≤ 23 −12 ≤ <i>k</i> ≤ 12 −8 ≤ <i>l</i> ≤ 8	−7 ≤ <i>h</i> ≤ 6 −18 ≤ <i>k</i> ≤ 18 −15 ≤ <i>l</i> ≤ 15
<i>μ</i> [mm <sup>-1</sup> ]	0.370	0.455	0.430	2.839
<i>F</i> (000)	320	1072	552	636
Independent data	2920	2280	2325	2026
Observed data [ <i>I</i> <sub>o</sub> > 2σ( <i>I</i> <sub>o</sub> )]	2530	1950	2285	1940
Parameters	191	128	200	137
Gof on <i>F</i> <sup>2</sup>	1.051	1.067	1.080	1.110
<i>R</i> , <i>R'</i> (all data)	0.0389, 0.0462	0.0309, 0.0398	0.0183, 0.0190	0.0221, 0.0232
w <i>R</i> , w <i>R'</i> (all data)	0.0993, 0.1056	0.0763, 0.0806	0.0470, 0.0477	0.0587, 0.0592

cal (H–C) or original (H–O,N) positions with thermal parameters  $U_{eq}(H) = 1.2 U_{eq}(C)$  or  $1.3 U_{eq}(N,O)$  as the free refinement led to unrealistic bond lengths and angles. Hydrogen atoms belonging to solvate thf molecule were fixed in theoretical positions using a riding model. In the structure of (NH<sub>4</sub>)<sub>3</sub>(Hmeth)·H<sub>2</sub>O, all hydrogen atoms were refined isotropically. In the structures of (NH<sub>4</sub>)(H<sub>3</sub>prop)·H<sub>2</sub>O and {[Cu<sub>2</sub>(H<sub>2</sub>pam)<sub>2</sub>]·H<sub>2</sub>O}<sub>n</sub>, the hydrogen atoms were localised in the electronic density difference map, but they were fixed in theoretical (H–C) or original (H–O,N) positions using a riding model with  $U_{eq}(H) = 1.2 U_{eq}(C)$  or  $1.3 U_{eq}(N,O)$  as the free refinement led to unrealistic bond lengths and angles. The independent unit of (NH<sub>4</sub>)(H<sub>3</sub>prop)·H<sub>2</sub>O consists of a ligand molecule, two ammonium cations occupying special positions (with half-occupancy) and one water molecule. In the other structures, no special positions are occupied. The non-centrosymmetric structure of (NH<sub>4</sub>)<sub>3</sub>(Hmeth)·H<sub>2</sub>O was refined with a contribution of racemic twinning with a ratio between both antipodes 62:38. CCDC-612685 (H<sub>4</sub>aca·thf), -612687 [(NH<sub>4</sub>)(H<sub>3</sub>prop)·H<sub>2</sub>O], -612686 [(NH<sub>4</sub>)<sub>3</sub>(Hmeth)·H<sub>2</sub>O] and -612688 {[Cu<sub>2</sub>(H<sub>2</sub>pam)<sub>2</sub>]·H<sub>2</sub>O}<sub>n</sub> contain the supplementary crystallographic data for this paper. These data can be obtained free of charge from The Cambridge Crystallographic Data Centre via [www.ccdc.cam.ac.uk/data\\_request/cif](http://www.ccdc.cam.ac.uk/data_request/cif).

#### Determination of Dissociation and Stability Constants

**Chemicals and Stock Solutions for Potentiometric Titrations:** Water was purified with a Milli-Q (Millipore) purification system. The stock solution of hydrochloric acid (ca. 0.03 M) was prepared from a 35% aqueous solution (puriss., Fluka). Commercial NMe<sub>4</sub>Cl (99%, Fluka) was recrystallised from boiling *i*PrOH and the solid salt was dried with P<sub>2</sub>O<sub>5</sub> in vacuo to constant weight (this dried salt is extremely hygroscopic).<sup>[36]</sup> Carbonate-free NMe<sub>4</sub>OH solution (ca. 0.2 M) was prepared from this NMe<sub>4</sub>Cl by ion exchange on Dowex 1 (OH<sup>−</sup> form, under argon, with carbonate-free water). The

hydroxide solution was standardised against potassium hydrogen phthalate and the HCl solution against the approx. 0.2 M NMe<sub>4</sub>OH solution. Stock solutions of the individual metal cations were prepared by dissolving hydrates of M(NO<sub>3</sub>)<sub>2</sub> or dried NaCl. The divalent metal ion contents in the stock solutions were determined by titration with standard Na<sub>2</sub>H<sub>2</sub>edta solution. The analytical concentration of ligand stock solution was determined together with refinement of protonation constants with the OPIUM<sup>[37]</sup> software package (see below).

**Potentiometric Titrations:** Titrations were carried out in a vessel thermostatted at 25.0 ± 0.1 °C, at an ionic strength *I* = 0.1 M (NMe<sub>4</sub>Cl) and in the presence of extra HCl in the pH range 1.7–11.9 (protonation constants and complex with Na<sup>+</sup>) using a PHM 240 pH-meter, a 2-mL ABU 900 automatic piston burette and a GK 2401B combined electrode (all from Radiometer, Denmark). For systems with divalent metal ions, a precipitate was usually present at pH's between about 4 and 9, so data for this region were not collected. The initial volume was 5 mL and the concentration of the ligand was about 0.004 M. L:M molar ratios of 1:10 (Na<sup>+</sup> system), 1:1, 2:1 and 1:2 (other systems) were used. Five parallel titrations were carried out for each ratio, with each titration consisting of 40–50 points. An inert atmosphere was ensured by constant passage of argon saturated with the vapour of the solvent used in the measurements.

The constants (with their standard deviations) were calculated with the program OPIUM.<sup>[37]</sup> This program minimizes the criterion of the generalized least-squares method using the calibration function

$$E = E_0 + S \log[H^+] + j_1[H^+] + j_2 K_w/[H^+]$$

where the additive term *E*<sub>0</sub> contains the standard potentials of the electrodes used and the contributions of inert ions to the liquid-junction potential, *S* corresponds to the Nernstian slope, the value

of which should be close to the theoretical value of 59.159 mV, and  $j_1[\text{H}^+]$  and  $j_2 K_w/[\text{H}^+] = j_2[\text{OH}^-]$  terms are contributions of the  $\text{H}^+$  and  $\text{OH}^-$  ions to the liquid-junction potential. The  $j_1$  and  $j_2$  parameters for the calibration titrations before and after each titration show only minor changes. It is clear that  $j_1$  (values between -50 and 50) and  $j_2$  (values between 100 and 200) cause deviation from a linear dependence between  $E$  and pH only in strongly acidic and basic solutions. The calibration parameters were determined by titration of standard HCl with standard  $\text{NMe}_4\text{OH}$  before each ligand or ligand-metal titration to give a pair calibration/titration, which was used for calculation of the constants. The protonation constants  $\beta_n$  are defined by  $\beta_n = [\text{H}_n\text{L}]/([\text{H}]^n[\text{L}])$  [they can be transferred to the dissociation constants by the relationships  $\text{p}K_a(\text{HL}^{3-}) = \log \beta_1$  and  $\text{p}K_a(\text{H}_n\text{L}^{n-4}) = \log \beta_n - \log \beta_{n-1}$ ]. The stability constants are defined by  $\beta_{hlm} = [\text{H}_h\text{L}_l\text{M}_m]/([\text{H}]^h[\text{L}]^l[\text{M}]^m)$ . The water ion product  $\text{p}K_w$  used was 13.81. The stability constants of  $\text{M}^{2+}\text{-OH}^-$  systems were included in the calculations and were taken from the literature.<sup>[21,38]</sup> Speciation of the studied systems was solved with the OPIUM<sup>[37]</sup> software package. The concentration of ligand supposed from the exactly weighed sample was in very good agreement with the concentration determined together with refinement of the protonation constants using OPIUM.

**NMR Titrations:** The  $^{31}\text{P}\{^1\text{H}\}$  NMR titration experiments for determination of the highest protonation constant (pH in range 11.5–13.6, about 15 points) were carried out under conditions close to the potentiometric titrations (no control of ionic strength,  $\text{NMe}_4\text{Cl}$ , 25.0 °C, ligand concentration about 0.004 M). A coaxial capillary tube with  $\text{D}_2\text{O}$  and  $\text{H}_3\text{PO}_4$  was used for the lock and referencing. Protonation constants were calculated with OPIUM<sup>[37]</sup> from the dependence of  $\delta_P$  of the phosphonate groups on  $-\log[\text{H}^+]$ .

**Supporting Information** (see also the footnote on the first page of this article): Discussion and experimental details dealing with the ligand synthesis. Figure S1 shows an example ( $\text{Na}^+:\text{H}_4\text{prop}$  system) of the fitting with and without hydroxo species. Table S1 shows the pH ranges skipped during titration due to the precipitate formation. Table S2 shows a comparison of the dissociation constant with those reported in the literature. The distribution diagrams of all systems studied are shown in Figures S2–S7. The hydrogen-bond parameters in the crystal structures are reported in Tables S3–S6.

## Acknowledgments

Support from the Grant Agency of the Czech Republic (no. 203/06/0467) and the Grant Agency of Academy of Science of the Czech Republic (no. KAN201110651; program “Nanotechnology for Society”) is acknowledged. This work was carried out in the framework of COST D38 and the NoE projects supported by the European Union, EMIL (no. LSHC-2004-503569) and DiMI (no. LSHB-2005-512146). We thank Ms. M. Malíková for her help with the titration experiments.

- [1] H. Fleisch, *Bisphosphonates in Bone Disease*, 4th ed., Academic Press London, 2000.
- [2] I. K. Adzamlı, D. Johnson, M. Blau, *Invest. Radiol.* **1991**, 26, 143–148.
- [3] I. K. Adzamlı, M. Blau, M. A. Pfeffer, M. A. Davis, *Magn. Reson. Med.* **1993**, 29, 505–511.
- [4] V. Kubiček, J. Rudovský, J. Kotek, P. Hermann, L. Vander Elst, R. N. Muller, Z. I. Kolar, H. T. Wolterbeek, J. A. Peters, I. Lukeš, *J. Am. Chem. Soc.* **2005**, 127, 16477–16485.
- [5] M. N. Rusina, T. M. Baleshova, B. V. Valeshov, A. J. Shitrina, I. A. Poljakova, *Zh. Obsch. Khim.* **1977**, 47, 1721–1726.

- [6] M. I. Kabashnik, T. J. Medved, N. M. Djatlova, J. M. Polikarpov, B. K. Sherbakov, F. I. Belskij, *Izv. Akad. Nauk Ser. Khim.* **1978**, 433–437.
- [7] J. E. Bollinger, D. M. Roundhill, *Inorg. Chem.* **1993**, 32, 2821–2826.
- [8] J. E. Bollinger, D. M. Roundhill, *Inorg. Chem.* **1994**, 33, 6421–6424.
- [9] M. Dyba, H. Kozłowski, A. Tlalka, Y. Leroux, D. E. Manouni, *Pol. J. Chem.* **1998**, 72, 1148–1153.
- [10] Z. H. Kudzin, A. Kotynski, G. Andriewski, *J. Organomet. Chem.* **1994**, 479, 199–205.
- [11] B. Boduszek, M. Dyba, M. Jezowska-Bojczuk, T. Kiss, H. Kozłowski, *J. Chem. Soc., Dalton Trans.* **1997**, 973–976.
- [12] S. V. Mamveev, F. I. Beljskii, A. G. Mamveeva, A. Yu. Gukaso, Yu. M. Polikarpov, M. Kabachnik, *Izv. Akad. Nauk Ser. Khim.* **1998**, 1784–1787.
- [13] M. Dyba, M. Jezowska-Bojczuk, E. Kiss, T. Kiss, H. Kozłowski, Y. Leroux, D. E. Manouni, *J. Chem. Soc., Dalton Trans.* **1996**, 1119–1123.
- [14] H. Wada, Q. Fernando, *Anal. Chem.* **1972**, 44, 1640–1643.
- [15] R. L. Carroll, R. R. Irani, *Inorg. Chem.* **1967**, 6, 1994–1998.
- [16] *Aminophosphonic and Aminophosphinic Acids: Chemistry and Biological Activity* (Eds.: V. P. Kukhar, H. R. Hudson), John Wiley & Sons, 2000.
- [17] K. Popov, H. Rönkkömäki, L. H. J. Lajunen, *Pure Appl. Chem.* **2006**, 78, 663–675.
- [18] E. Matczak-Jon, B. Kurzak, P. Kafarski, A. Wozna, *J. Inorg. Biochem.* **2006**, 100, 1155–1166.
- [19] I. Lukeš, J. Kotek, P. Vojtišek, P. Hermann, *Coord. Chem. Rev.* **2001**, 216–217, 287–312.
- [20] T. G. Appleton, J. R. Hall, A. D. Harris, M. A. Kimlin, I. J. Mc Mahon, *Aust. J. Chem.* **1984**, 37, 1833.
- [21] A. E. Martell, R. M. Smith, *Critical Stability Constants*, Plenum Press, New York, **1974–1989**, vol. 1–6; *NIST Standard Reference Database 46 (Critically Selected Stability Constants of Metal Complexes)*, Version 7.0, **2003**.
- [22] E. Matczak-Jon, V. Videnova-Arabinska, *Coord. Chem. Rev.* **2005**, 249, 2458–2488.
- [23] E. Tillmanns, W. H. Baur, *Inorg. Chem.* **1970**, 9, 1957–1958.
- [24] N. N. Greenwood, A. Earnshaw, *Chemistry of the Elements*, Pergamon Press Plc, Oxford, **1984**.
- [25] J. A. Cowan, *Inorganic Biochemistry*, VCH Publishers, Inc., New York, **1993**.
- [26] A. W. Addison, T. N. Rao, J. Reedijk, J. van Rijn, G. C. Verschoor, *J. Chem. Soc., Dalton Trans.* **1984**, 1349–1356.
- [27] H. Song, L. Zheng, Y. Liu, X. Xin, A. J. Jacobson, S. Decurtins, *J. Chem. Soc., Dalton Trans.* **2001**, 3274–3278.
- [28] Z. C. Hu, H. Y. Wei, Z. D. Chen, *J. Mol. Struct.* **2004**, 668, 235–242.
- [29] G. R. Kieczkowski, D. F. Jobson, D. G. Melillo, D. F. Reinhold, V. J. Grenda, I. Shinkai, *J. Org. Chem.* **1995**, 60, 8310–8312.
- [30] D. Kantoci, J. K. Denike, W. J. Wechter, *Synth. Commun.* **1996**, 26, 2037–2043.
- [31] W. Winckler, T. Pieper, B. K. Keppler, *Phosphorus Sulfur Siliol. Relat. Elem.* **1996**, 112, 137–141.
- [32] Z. Otwinowski, W. Minor, *HKL Denzo and Scalepack Program Package* by Nonius BV, Delft, **1997**; For a reference see: Z. Otwinowski, W. Minor, *Methods Enzymol.* **1997**, 276, 307–326.
- [33] A. Altomare, M. C. Burla, M. Camalli, G. Casciarano, C. Giacovazzo, A. Guagliardi, G. Polidori, *J. Appl. Crystallogr.* **1994**, 27, 435.
- [34] G. M. Sheldrick, *SHELXL97: Program for Crystal Structure Refinement from Diffraction Data*, University of Göttingen, Germany, **1997**.
- [35] P. Coppens, *Crystallographic Computing*, Munksgaard, Copenhagen, **1970**, p. 255.
- [36] P. Táborský, P. Lubal, J. Havel, J. Kotek, P. Hermann, I. Lukeš, *Collect. Czech. Chem. Commun.* **2005**, 70, 1909–1942.

- [37] M. Kývala, I. Lukeš, *International Conference on Chemometrics* 95, p. 63. Pardubice, Czech Republic, **1995**; the full version of OPIUM is available (free of charge) from <http://www.natur.cuni.cz/~kyvala/opium.html>.
- [38] C. F. Baes Jr., R. E. Mesmer, *The Hydrolysis of Cations*, Wiley, New York, **1976**.

Received: June 29, 2006

Published Online: November 3, 2006